Science Advances

AAAS

advances.sciencemag.org/cgi/content/full/4/2/e1700682/DC1

Supplementary Materials for

Dipole-like electrostatic asymmetry of gold nanorods

Ji-Young Kim, Myung-Geun Han, Miao-Bin Lien, Sergei Magonov, Yimei Zhu, Heather George, Theodore B. Norris, Nicholas A. Kotov

Published 9 February 2018, *Sci. Adv.* **4**, e1700682 (2018)
DOI: 10.1126/sciadv.1700682

This PDF file includes:

Supplementary Materials

Gold chloride trihydrate ($HAuCl_4$, Cat.# 520918), silver nitrate ($AgNO_3$, Cat.# 204390), trisodium citrate dihydrate (Cat.# S4641), sodium borohydride ($NaBH_4$, Cat.# 480886), poly(sodium 4-styrenesulfonate) (PSSS, Mw = 1,000,000, Cat.# 434574), Poly(vinyl alcohol) (PVA, Mw=85,000-124,000, Cat. # 363146), Poly(diallyldimethylammonium chloride) solution (20 wt.%, Cat# 409014), cetyltrimethylammonium bromide (CTAB, Cat# H9151) and ascorbic acid (Cat.# A7506) were purchased from Sigma-Aldrich (Milwaukee, WI). The quartz slide (Prod # 26013) and ultrathin carbon film on lacey carbon support film, 400 mesh, copper (Prod # 01824) were purchased from Ted Pella (Redding, CA). Non-Porous Pure Silicon 5 nm thick TEM windows (Cat.# US100-A05Q33A) were purchased from TEMwindows.com. Ultrapure water from a Direct-Q3 system (18.2 MΩ·cm, Millipore; Billerica, MA) was used in this work.

Supplementary Methods

Grazing incident X-ray diffraction (GiXRD) measurement: GiXRD patterns from film samples were obtained using a Rigaku Ultima IV X-Ray diffractometer. To prepare the nearly horizontally-aligned AuNR sample, the bare AuNR colloid was spin-coated on a quartz slide. The same PSS/AuNR and reference samples for which we measured nonlinear optical responses were used to obtain their GiXRD patterns. All measurements were taken at 40 kV and 44 mA.

Ligand exchange of CTAB on AuNRs with PSS and PVA: The concentrated CTAB-AuNR solution (3 OD) after the purification step was redispersed in 1 mL of 2 wt% PSS and PVA solutions, respectively. After 30 min stirring in room temperature, the solutions were centrifuged down (8000 rpm, 25 min) and redispersed in DDI water. After 3 minutes vigorous stirring, the solutions are re-centrifuged down (4000 rpm, 10 min) and redispersed in 100 µL of DDI water to obtain purified concentrated AuNR solutions.

X-ray Photoelectron Spectroscopy (XPS) Analysis: The concentrated solution was drop-casted on indium foil for XPS analysis. The spectrum mode using the monochromated Al source was used to survey the energy range from 0 to 600 eV with energy resolution ~0.5 eV using a Kratos Axis Ultra X-ray photoelectron spectrometer.

Supplementary Discussion

Computational Analysis of Plasmon Mode Shift from Local Environment

Different plasmon modes of silver nanowires (AgNWs) were computed using the wave-optics module of COMSOL Multiphysics 5.1. The model was constructed based on the actual size of the silver nanowire (width: 15 nm and length: 375 nm) shown in previous literature (8). A series of plane-polarized electromagnetic waves traveling perpendicularly into the long axis of the AgNWs were applied to calculate electric fields of plasmon modes of NWs with/without spherical particles located along the long axis with a 20 nm gap. The shifts of the plasmon center by the neighboring spherical particle are negligible for all modes (from

500 nm to 1500 nm with 250 nm intervals, Extended Data Fig. 1a and b), and therefore suggest that the significant mode shift observed in the literature (17 nm) is unlikely to be generated by the local environment. We only observed a small intensity asymmetry for higher plasmon modes (wavelength = 500 nm, fig. S1C).

Element Analysis of AuNR after Ligand Exchange of CTAB with PSS and PVA

To investigate the affinity of PSS and PVA on a gold surface during film sample preparation for optical property measurement, we examined the yield of CTAB ligand exchange for PSS and PVA as colloids. The AuNRs collected from PSS solution had negligible nitrogen peaks (fig. S3A), which proves chemically that the CTAB layers on the AuNRs had been effectively removed during the LBL process with PSS. In contrast, the sample from PVA had a nitrogen peak (fig. S3B), which indicates that only a passivation had occurred in PVA solution with a continued presence of CTAB layer on gold. Thus we can conclude that the CTAB layer of AuNRs is preserved in PVA/AuNR composites, maintaining the asymmetric charge distribution.

Orientation of AuNRs in film samples

The orientation of AuNRs in a polymer matrix could be one of the factors for the efficiency of nonlinear optical properties due to different likelihood of resonance or retardation. For instance, if all AuNRs are parallel to the surface of the quartz slide, thus perpendicularly oriented to the incident beam direction, the retardation effect would be minimized, and depression of SHG is not surprising in this case. To confirm that our observation of SHG depression shown in Fig. 5E is not caused by the arrangement of AuNRs, we analyzed a grazing incident X-ray diffraction (GiXRD) pattern (fig. S6B) of a PSS/AuNR composite film. Compared with the GiXRD pattern of horizontally aligned AuNRs, AuNRs embedded in a PSS LBL matrix with spacer show weaker relative peaks for the side facet of AuNRs (200). This proves that the AuNRs in the LBL matrix are not horizontally aligned, thus depression of SHG cannot be attributed to the lesser retardation likelihood of AuNRs in the film. The direct observation of the surface of the PSS/AuNR film by SEM imaging also indicates the existence of AuNRs having almost perpendicular orientations to the quartz substrate (fig. S6C).

CTAB removal test with electron beam treatment:

To investigate how a focused electron beam (*e* - beam) removes the CTAB layer, the intensity of SEM for a thick CTAB deposition area with exposure time to the e^- beam of 10 min was recorded (fig. S4A). 10 min of e^- beam treatment removed approximately 20 percent of the CTAB, thus demonstrating the partial removal of CTAB on AuNRs by *e* - beam processing.

Computational Analysis of Plasmon Mode Shift from asymmetrical geometry of AuNR:

We commutated Plasmon intensities ratio changes derived by geometrical asymmetry to examine if the intensity asymmetry observed in EELS map can be considered significant. We

constructed two model of AuNRs with perfect centrosymmetry and asymmetry with the eccentricity of 0.6, and computed their plasmon map at the longitudinal resonance condition using Lumerical FDTD solution (fig. S7). Even with this significant geometrical asymmetry, the integrated intensity ratio of the same area was found to be about 8 %, smaller than observed in EELS experimental result. Moreover, our plasmon map computation with adjunct particle (fig. S1) also showed that local environment cannot rationalize the observed asymmetry. We believe that there must be a major contribution of electrostatic asymmetry by CTAB patchiness to this Plasmon asymmetry, possibly 10 % out of 12.5 % considering corrected intensity ratio after e-beam treatment.

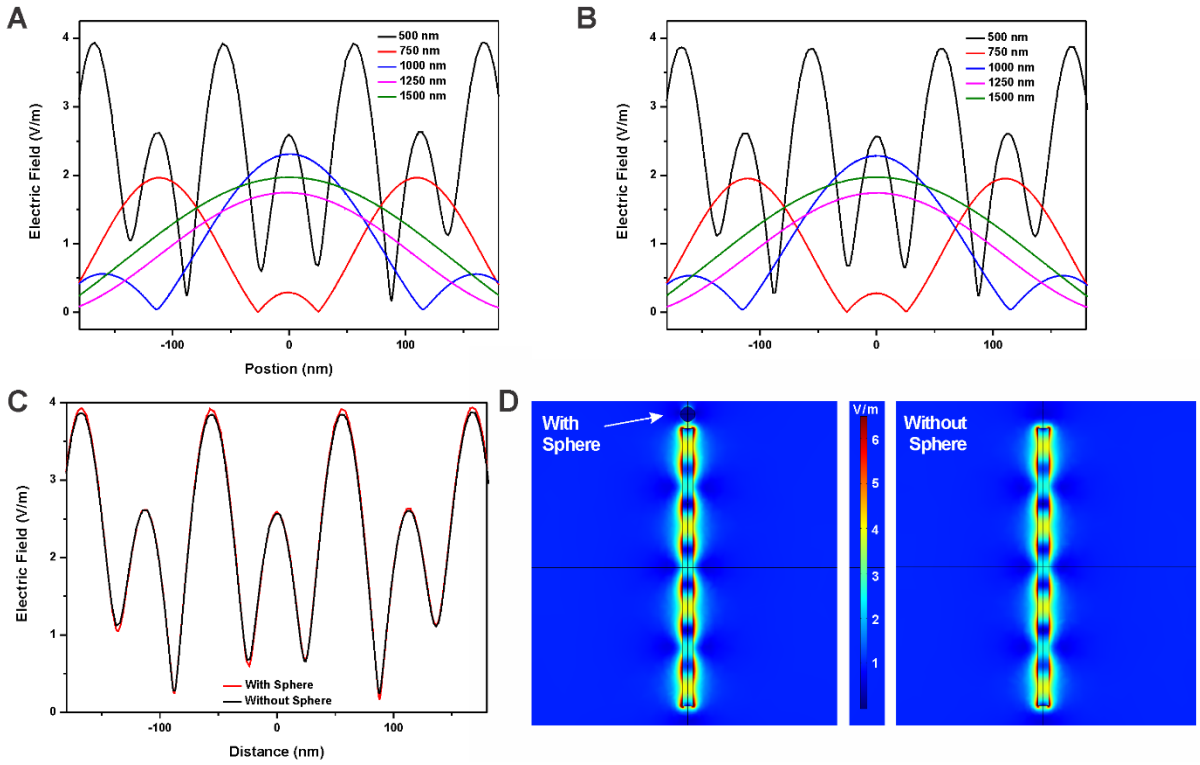

fig. S1. Computations of plasmon modes of silver nanowire (NW) with and without a neighbor particle. Electric field profile along NW long axis with (**A**) /without (**B**) a neighbor sphere interacting with different wavelengths of plane-polarized waves. A comparison of two plasmon line profiles (**C**) and images (**D**) for the wavelength of 500 nm.

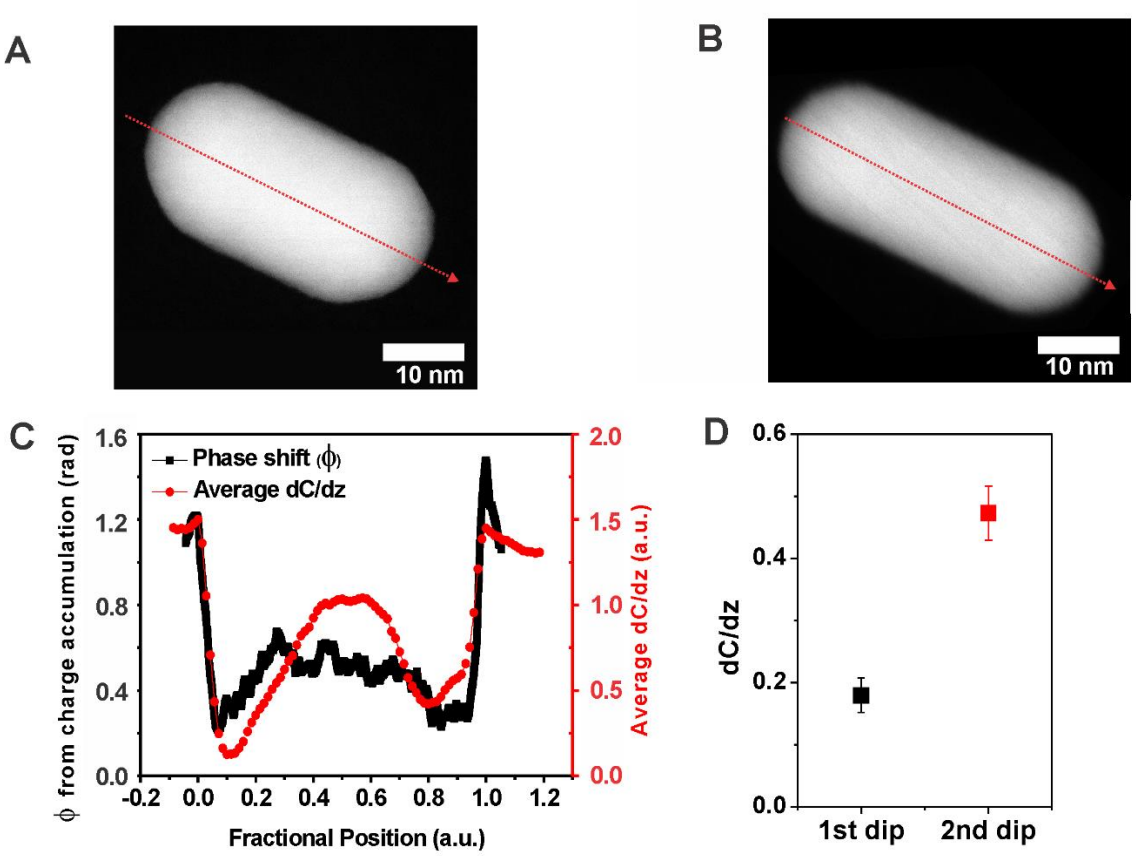

fig. S2. HAADF images of AuNRs and analysis of capacitance gradient (dC/dz) profiles obtained by Kelvin probe microscopy. (**A, B**) HAADF images of AuNRs presented in Fig. 1a and 1c in main text, respectively. (**C**) The phase shift caused by accumulated charge potential of AuNR (black) observed by electron holography and average dC/dz profile of AuNRs (red) taken by Kelvin probe microscopy. (**D**) Comparison of two dips shown in the capacitance gradient profile of individual AuNRs at their termini. Data represent mean ± SEM, n = 9. The difference is considered statistically significant with p value = 0.0002.

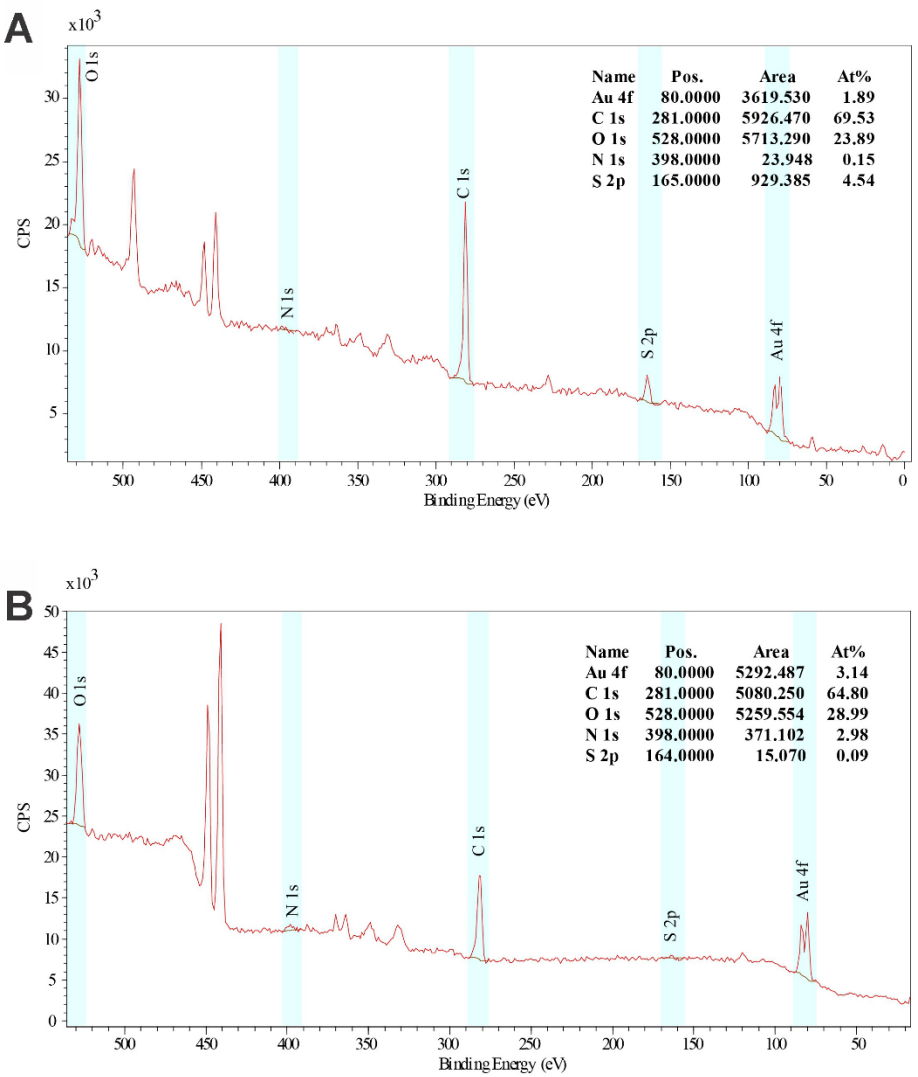

fig. S3. Ligand exchange of CTAB on AuNRs with PSS and PVA. XPS spectra of purified AuNRs after being dispersed in highly concentrated PSS (**A**) and PVA (**B**), respectively.

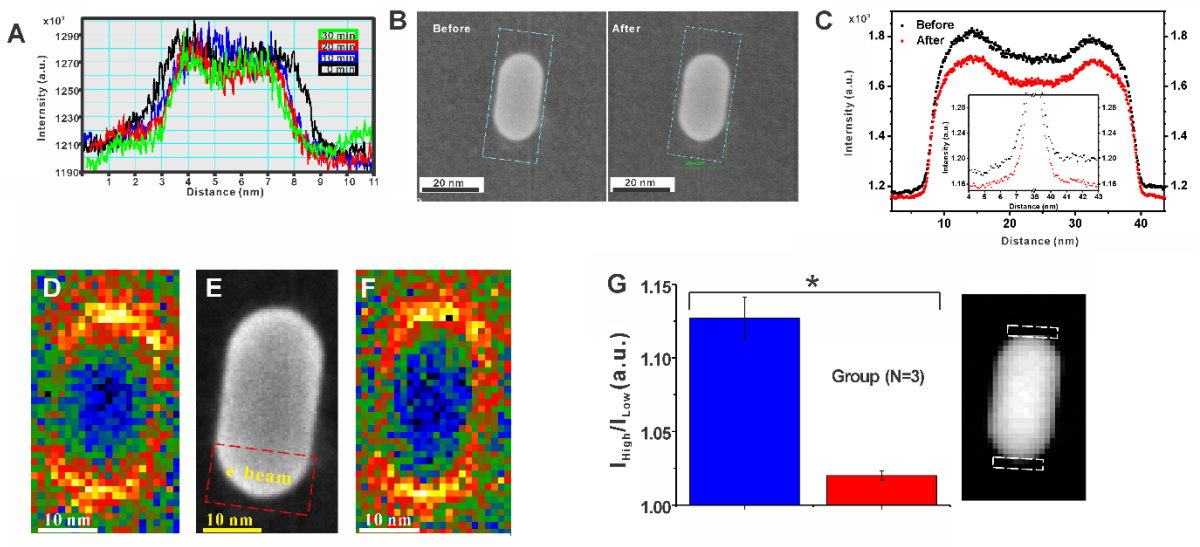

fig. S4. *e*-beam ablation for selective removal of CTAB on single AuNRs and their plasmon mapping. (**A**) SEM intensity difference of highly concentrated CTAB bridges between two AuNRs for different durations of *e*-beam ablation. (**B**) SEM images and (**C**) intensity line profile of AuNRs (for light blue box area, with direction from top to bottom) before/after *e*-beam ablation. **. (D, F)** EELS mapping for the range of 1.8 eV-2.2 eV (longitudinal plasmon) before and after electron beam treatment, respectively. A paired t-test for these EELS data was performed; by conventional criteria, this difference of the intensity ratio between before and after treatments is considered to be statistically significant (p value = 0.015). (**E**) SEM image for the same AuNR with a red box indicating the area of electron beam ablation for 5 minutes. (**G**) Ratio between integrated intensities for two resonance poles before (blue) and after (red) electron beam treatment, respectively. Data represent mean ± standard error of mean (SEM), n=3. Integrated area is identified with white dashed box in image of AuNR (right).

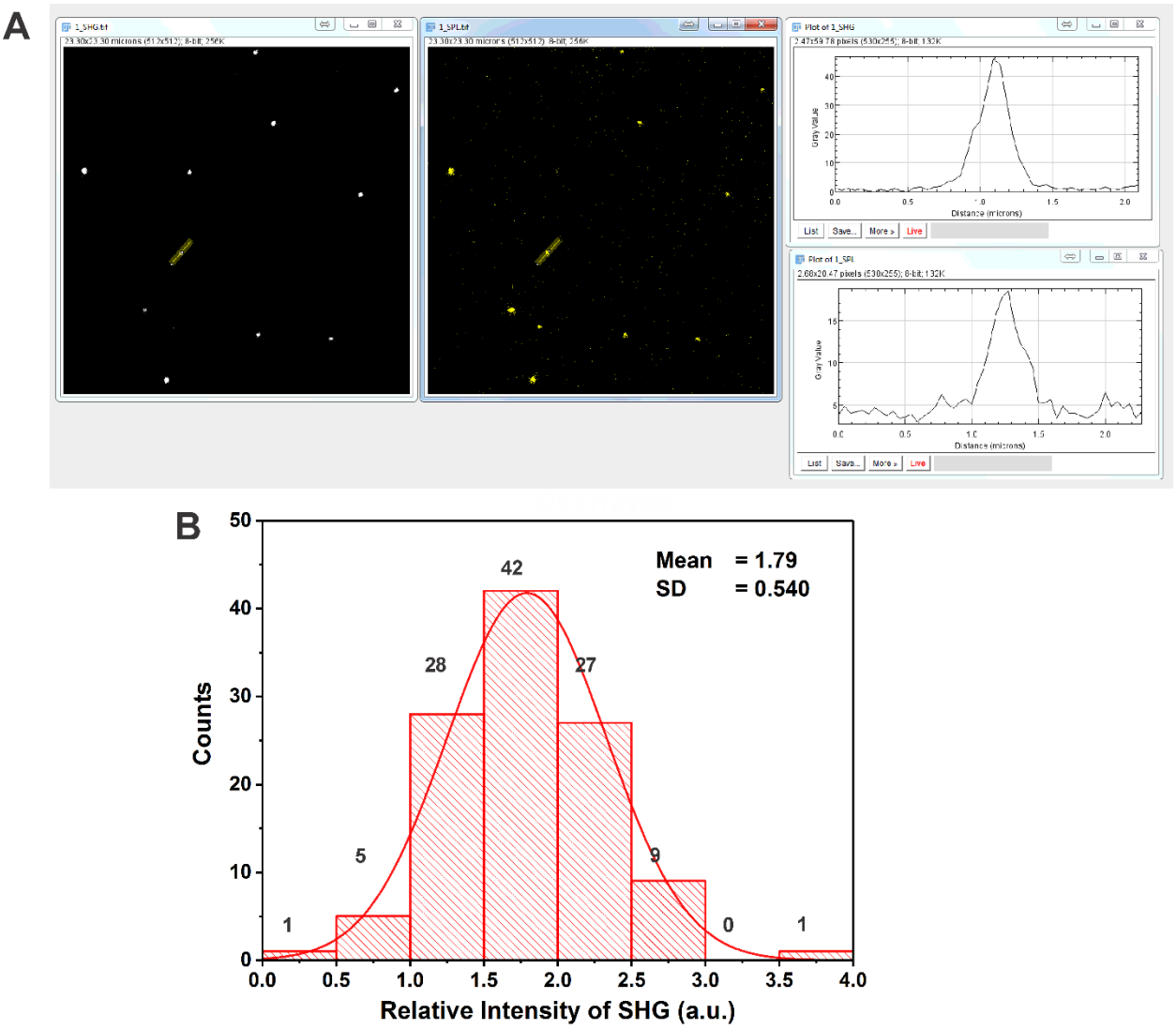

fig. S5. Intensity of individual AuNRs in SHG- and FL-mode imaging. (A) Signal-to-noise ratio difference between SHG and FL images of AuNRs. **(B)** Distribution analysis of relative SHG intensity to FL. No significant departure from normality was found in normality test (p value =0.078 > 0.05)

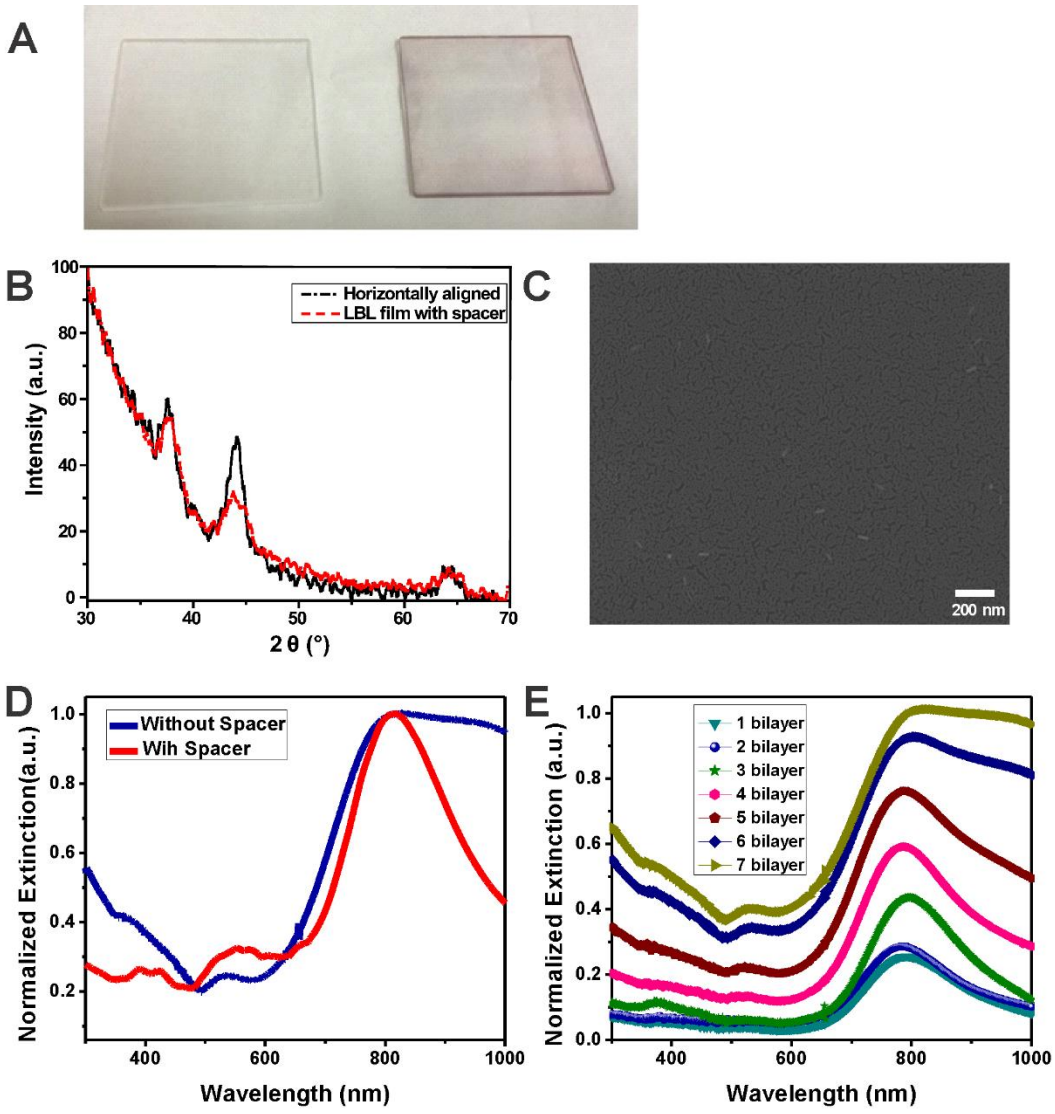

fig. S6. LBL-assembled AuNR/PSS films. (**A**) Sample picture of decoupled AuNR composite and reference polymer film on quartz slides. (**B**) Grazing incident X-ray diffraction (GiXRD) measurement of decoupled AuNR composite and spin-coated AuNR quartz slides. (**C**) SEM image showing top-view of decoupled AuNR composite film. (**D**) UV-vis spectra of AuNR composite film with/without spacer. (**E**) UV-vis spectra change of coupled AuNR composites by addition of AuNR/PSS bilayers.

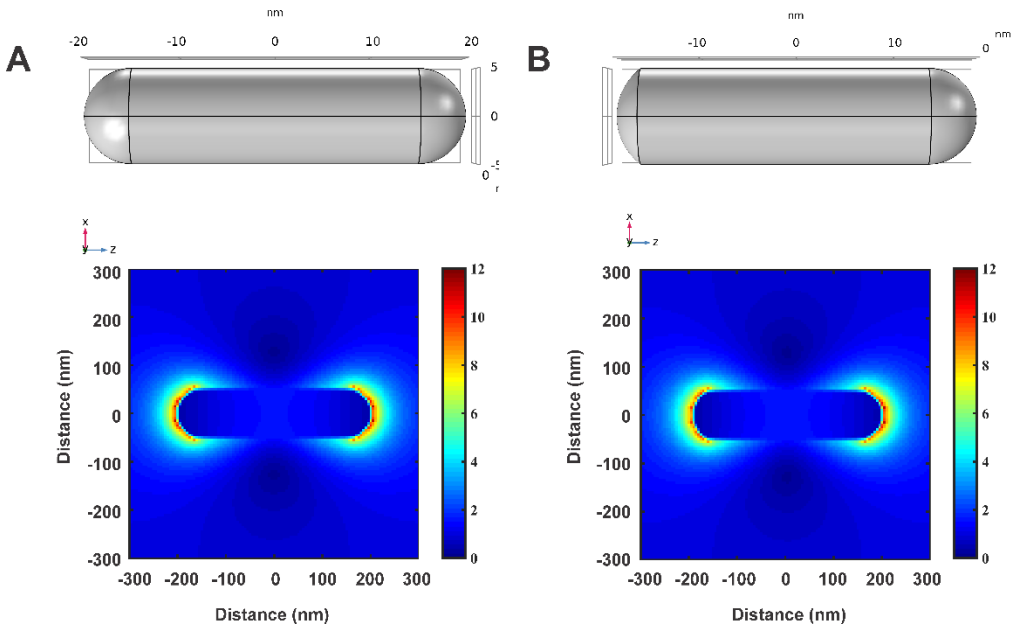

fig. S7. Computation of plasmon modes of AuNRs with and without centrosymmetrical gold core geometry. (A) Plasmon map (bottom) at resonance condition, 808 nm, with perfect centro-symmetric AuNR model (top). (B) Plasmon map (bottom) at resonance condition, 808 nm, with asymmetric AuNR model with one end cap having the eccentricity of 0.6 (top).